# Investigation of the Skewing of the slots in Permanent Magnet Synchronous Machines

Tsvetomir Stoyanov
*General Electrical Engineering*
*Technical University of Sofia*
Sofia, Bulgaria
cmetodiev@tu-sofia.bg

Radoslav Spasov
*Electrical Machines*
*Technical University of Sofia*
Sofia, Bulgaria
rls@tu-sofia.bg

Plamen Rizov
*Electrical Machines*
*Technical University of Sofia*
Sofia, Bulgaria
pmri@tu-sofia.bg

***Abstract*— This paper presents a study of slot skewing in a permanent magnet synchronous motor. Several cases are considered where the rotor is divided into multiple segments. The segmentation is done in the area between two stator slots. Three segmentations were performed in order to obtain more accurate results while saving computing time. A 2D model based on finite element method was used instead of a 3D one due to the requirement of low computing time. The accuracy of the solution is not significantly affected due to the selection of a 2D model. Different types of segmentations are used to evaluate the maximum value of the main harmonic of electromotive force and air-gap torque. The studies were performed for three different values of current density.**

***Keywords*— permanent magnet synchronous motor, rotor segmentations, 2D model, air-gap torque, permanent magnet position, current density.***

## I. INTRODUCTION

The power of electrical motors used in electrical drives ranges from a few watts to several megawatts. They are used to drive a wide variety of machines and equipment in transport and industry as well as in the home. Until recently the leading type of motors used for electrical drives has been the induction motor. The trend in the recent years has been to replace induction motors with permanent magnet synchronous motors[7]. Generally these motors are more efficient than induction motors. This leads to the increased research interest into the design of a new generation of permanent magnet synchronous motors with high technical performance, taking into account the disadvantages of this type of motor. One such disadvantage is the price of permanent magnets. Improving the efficiency for the same permanent magnet volume is of particular importance. This can be achieved through a variety of motor configurations and selection of a suitable inverter and control methods [1, 8]. The selection of configuration, magnet sizes and control algorithm is usually made before the motor is manufactured. There are a number of methods for this purpose, one commonly used being the finite element method. In this method the study area is broken down into many smaller elements.

Part of the principal construction of the permanent magnet synchronous motor is shown on Fig.1. This construction is often used in hybrid and electric vehicles from bicycles to trucks. The maximum efficiency is the most important factor for such applications since some or all of the electrical energy is sourced from an autonomous battery located on the vehicle. For this reason improving efficiency by even a part of the percentage is a very important from a technical and economic point of view.

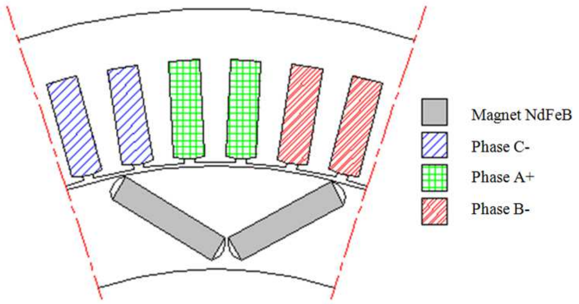

Fig. 1. Part of principal construction.

The article covers the following sections:

- Data about rotor's and stator's dimensions;
- Data about stator's winding;
- Selected methodology for simulating skewing of the slots;
- testing for different skewing and current densities;
- results;
- conclusions.

## II. MOTOR CONFIGURATION

The 3D view with corresponding dimensions of the part is shown on Fig.2. The values of the displayed dimensions and some machine parameters are presented in Table 1.

The diagram for the first twelve slots of the winding in the stator is shown on Fig.3. The arrangement of the stator winding in all the slots of the motor is shown on Fig.4. The

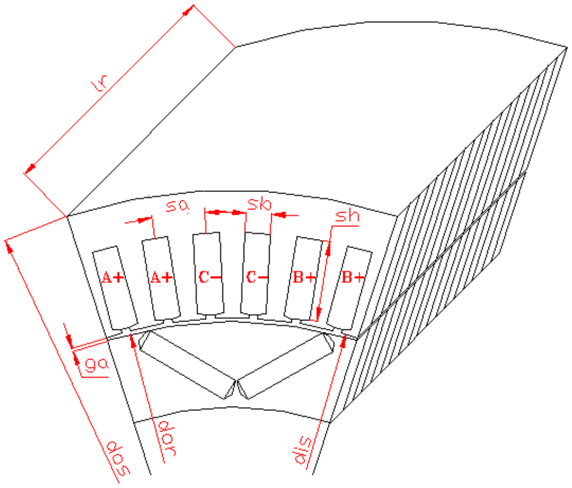

Fig. 2. Motor configuration

978-1-7281-9439-4/20/$31.00 ©2020 IEEE

connection between the different coils of the winding is presented on Fig.5.

TABLE I. DIMENSIONS AND SOME MOTOR PARAMETERS

| | | |
|---|---|---|
| Srator's slots Z | 60 | - |
| Pfase | 3 | - |
| Coil pith | 6 | - |
| Layers | 1 | - |
| ga | 0.70 | mm |
| lr | 90.0 | mm |
| sa | 30 | deg |
| sb | 5.80 | mm |
| sh | 18.10 | mm |
| dos | 242.0 | mm |
| dis | 184.20 | mm |
| dor | 182.80 | mm |

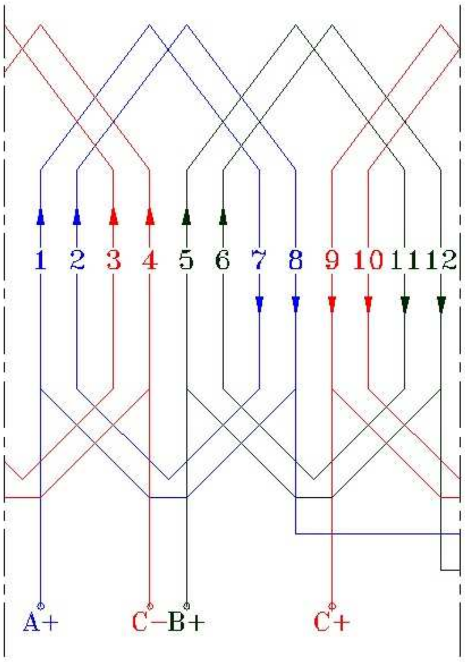

Fig. 3. Diagram for the first twelve slots of the winding.

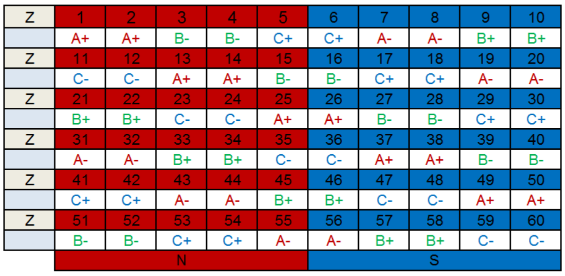

| Z | 1 | 2 | 3 | 4 | 5 | 6 | 7 | 8 | 9 | 10 |
|---|---|---|---|---|---|---|---|---|---|---|
| | A+ | A+ | B- | B- | C+ | C+ | A- | A- | B+ | B+ |
| Z | 11 | 12 | 13 | 14 | 15 | 16 | 17 | 18 | 19 | 20 |
| | C- | C- | A+ | A+ | B- | B- | C+ | C+ | A- | A- |
| Z | 21 | 22 | 23 | 24 | 25 | 26 | 27 | 28 | 29 | 30 |
| | B+ | B+ | C- | C- | A+ | A+ | B- | B- | C+ | C+ |
| Z | 31 | 32 | 33 | 34 | 35 | 36 | 37 | 38 | 39 | 40 |
| | A- | A- | B+ | B+ | C- | C- | A+ | A+ | B- | B- |
| Z | 41 | 42 | 43 | 44 | 45 | 46 | 47 | 48 | 49 | 50 |
| | C+ | C+ | A- | A- | B+ | B+ | C- | C- | A+ | A+ |
| Z | 51 | 52 | 53 | 54 | 55 | 56 | 57 | 58 | 59 | 60 |
| | B- | B- | C+ | C+ | A- | A- | B+ | B+ | C- | C- |
| | N | | | | | S | | | | |

Fig. 4. Arrangement of the stator winding in all the slots of the motor.

| A | B | C | coil |
|---|---|---|---|
| 1 | 9 | 5 | 1 |
| 7 | 15 | 11 | |
| 2 | 10 | 6 | 2 |
| 8 | 16 | 12 | |
| 13 | 21 | 17 | 3 |
| 19 | 27 | 23 | |
| 14 | 22 | 18 | 4 |
| 20 | 28 | 24 | |
| 25 | 33 | 29 | 5 |
| 31 | 39 | 35 | |
| 26 | 34 | 30 | 6 |
| 32 | 40 | 36 | |
| 37 | 45 | 41 | 7 |
| 43 | 51 | 47 | |
| 38 | 46 | 42 | 8 |
| 44 | 52 | 48 | |
| 49 | 57 | 53 | 9 |
| 55 | 3 | 59 | |
| 50 | 58 | 54 | 10 |
| 56 | 4 | 60 | |

Fig. 5. Connection between the different coils of the winding.

## III. ANALYSIS

By skewing of the slots, while maintaining the volume of the magnets, it is possible to achieve improvement of the motor's characteristics. It is possible to reduce the noise, vibrations, cogging torque and torque ripple. [3,5,6]. A number of authors present a methodology for optimal skewing of the slots [2,4,6]. This article borrows some ideas that are tailored to the particular construction of the motor. The research has taken into account the fact that with increasing the number of segments that the stator is divided into, the number of solutions increases significantly and hence the computational time. Due to the use of the 2D model, skewing of the slots was done by simulation to save computing time. First, a magnetic field solution was obtained for a motor without skewing of the slots and for a period of twenty milliseconds. Electromotive force and air-gap torque were calculated. The rotor is then rotated clockwise direction with a specified step „s"( geometric degrees). At the end the rotor is rotated in the opposite direction from the original position. The rotation of the rotor to obtain three zones "zn" is shown on Fig.6 The used steps are s =0.75 deg., s =1.5 deg., s =3.0 deg. Thus, the distance between two stator slot (which is six degrees) can be divided into a certain number of zones. The ratio between the number of steps and the number of zones is presented in Table 2. Studies have been carried out for different current densities ranging from 10 A/mm$^2$ to 30 A/mm$^2$. The electromotive force and air-gap torque are calculated as their value for each rotor position divided by the number of positions and then added up.

TABLE II. RATIO BETWEEN THE NUMBER OF STEPS AND THE NUMBER OF ZONES

| s | zn |
|---|---|
| 0.75 | 9 |
| 1.5 | 5 |
| 3 | 3 |

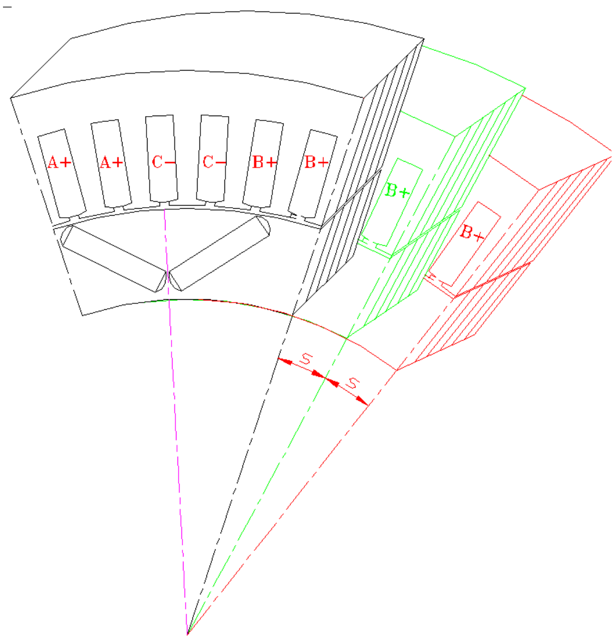

Fig. 6. Rotation of the rotor to obtain three zones..

The results obtained for the harmonic order of electromotive force and air-gap torque are shown from Fig.7 to Fig.8 for 10 A/mm$^2$. Similar dependencies for 20 A/mm$^2$- from Fig.9 to Fig.10; for 30 A/mm$^2$- from Fig.11 to Fig.12. The air-gap torque as time function is presented on Fig.13 to Fig.15. The main harmonics of electromotive force and air-gap torque are presented in Table 3.

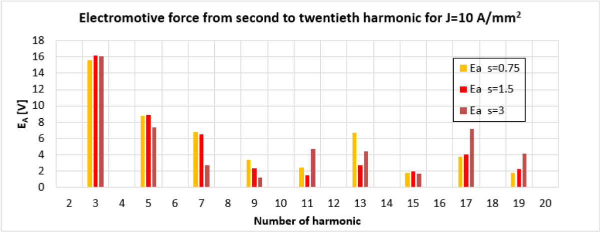

Fig. 7. The order of the e.m.f. harmonics at 10 A/mm$^2$.

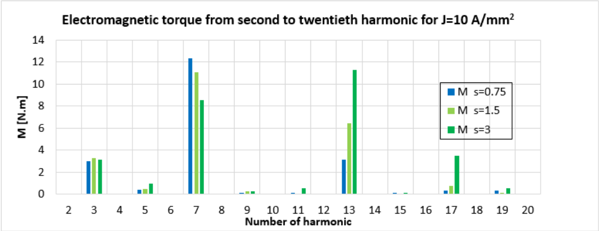

Fig. 8. The order of the torque harmonics at 10 A/mm$^2$.

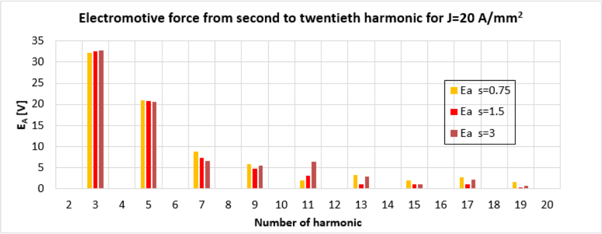

Fig. 9. The order of the e.m.f. harmonics at 20 A/mm$^2$.

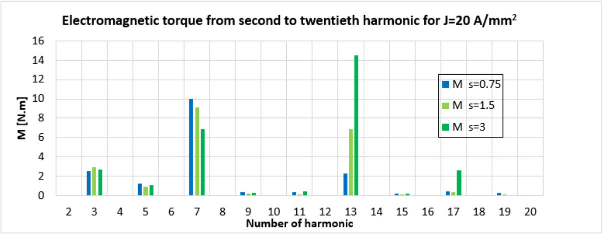

Fig. 10. The order of the torque harmonics at 20 A/mm$^2$.

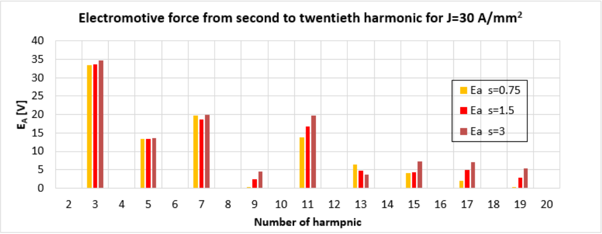

Fig. 11 The order of the e.m.f. harmonics at 30 A/mm$^2$.

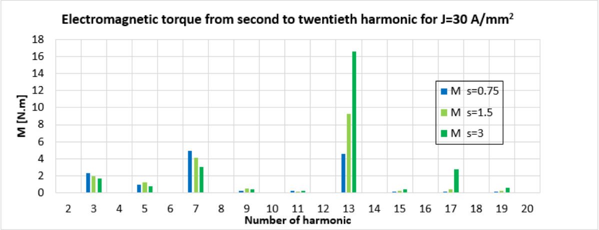

Fig. 12. The order of the torque harmonics at 30 A/mm$^2$.

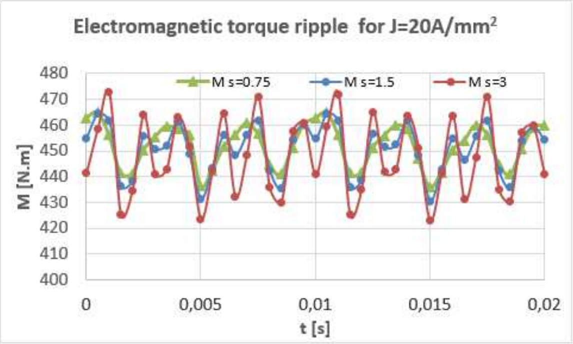

Fig. 14. Change of the moment for a period of time at 20 A/mm$^2$.

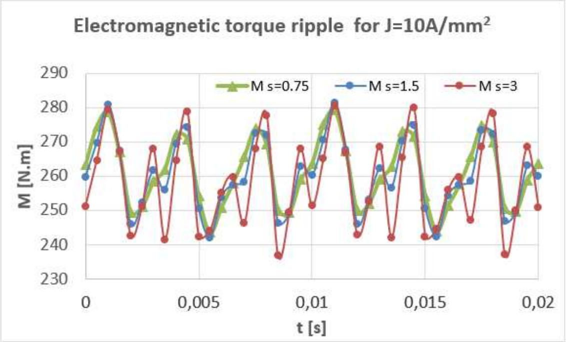

Fig. 13. Change of the moment for a period of time at 10 A/mm$^2$.

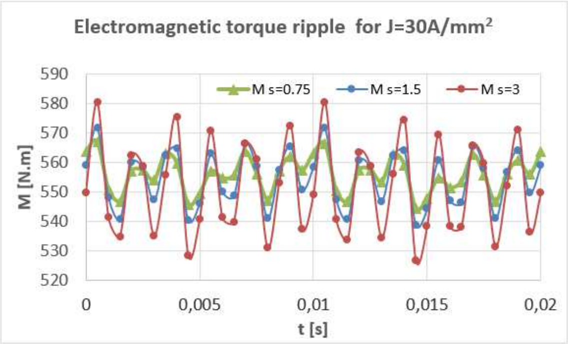

Fig. 15. Change of the moment for a period of time at 30 A/mm$^2$.

TABLE III. THE MAIN HARMONICS OF ELECTROMOTIVE FORCE AND AIR-GAP TORQUE

| Ea [V] | | | |
|---|---|---|---|
| J[A/mm$^2$] | 10 | 20 | 30 |
| s=3 | 307.3 | 354.9 | 390.3 |
| s=1.5 | 310.1 | 356.3 | 390.3 |
| s=0.75 | 313.4 | 357.3 | 390.7 |
| | | | |
| M [N.m] | | | |
| J[A/mm$^2$] | 10 | 20 | 30 |
| s=3 | 258.0 | 448.9 | 551.2 |
| s=1.5 | 260.3 | 450.6 | 554.5 |
| s=0.75 | 261.3 | 451.9 | 555.8 |

## IV. CONCLUSIONS

Investigation of slot skewing in permanent magnet synchronous motors is presented in this article to improve machine performance. The distance between two stator slots (which is six degrees) was divided into a certain number of zones. Studies have been carried out for different current densities. Increasing the number of zones leads to an increase in computing time. The electromotive force and air-gap torque are calculated as their value for each rotor position divided by the number of positions of the rotor. The optimal step for the study is “s=1.5”. The increase in the number of zones also leads to an increase in the ripple of air-gap torque (Fig.13 to Fig.15).

In conclusion it can be said that the minimum number of zones is three and the maximum depends on the time available to solve the problem.

## ACKNOWLEDGMENT

The authors would like to thank the Research and Development Sector at the Technical University of Sofia for the financial support.

## REFERENCES

[1] E. Rachev, V. Petrov, Mastering the transient process of switching from scalar to vector control for smooth startup of a synchronous permanent magnet motor, 11th Electrical Engineering Faculty Conference, 2019.

[2] F. Bahrim, E. Sulaiman, R. Kumar, L. Jusoh, New cogging torque reduction methods for permanent magnet machine, International Research and Innovation Summit (IRIS2017), https://iopscience.iop.org/article/10.1088/1757-899X/226/ 1/012127/pdf.

[3] J. Besnerais, Q. Souron, Design of quiet permanent magnet synchronous electrical motors by optimum skew angle, 23rd International congress on sound and vibration, 2016, https://eomys.com/IMG/pdf/design_of_quiet_permanent_magnet_synchronous_electrical_motors_by_optimum_skew_angle.pdf.

[4] K. Abbaszadeh, F. Alam, S. Saied, Cogging torque optimization in surface-mounted permanent-magnet motors by using design of experiment, Energy Conversion and Management 52 (2011), https://reader.elsevier.com/reader/sd/pii/S0196890411001397?token=84DAAD6A82D4063BFD8C0EC0C3D11564DB70C46B696B9DA83CD940E80DD69F8F6DCAA3515BB70316C8B07EC2C8C62147.

[5] L. Melcescu, M. Covrig, A. Moraru, analyses of core skewing influence in permanent magnet synchronous machine by 2d fem field computation, 2006, https://www.scientificbulletin.upb.ro/rev_docs_arhiva/full44720.pdf.

[6] N. Levin1, S. Orlova, V. Pugachov, B. Ose-Zala, E. Jakobsons, Methods to reduce the cogging torque in permanent magnet synchronous machines, Elektronika ir elektrotechnika, ISSN 1392-1215, VOL. 19, NO. 1, 2013, https://www.researchgate.net/publication/274432066_Methods_to_Reduce_the_Cogging_Torque_in_Permanent_Magnet_Synchronous_Machines.

[7] R. Ni, D. Xu, G. Wang, L. Ding, G. Zhang, L. Qu, Maximum efficiency per ampere control of permanent-magnet synchronous machines, IEEE TRANSACTIONS ON INDUSTRIAL ELECTRONICS, VOL. 62, NO. 4, APRIL 2015, https://www.researchgate.net/profile/Ron_ Ni/publication/ 273341847_Maximum_Efficiency_Per_Ampere_Control_of_Permanent Magnet_Synchronous_Machines/links/554d5d0c08 aeedf 175638b99/ Maximum-Efficiency-Per-Ampere-Control-of-Permanent-Magnet-Synchronous-Machines.pdf.

[8] V. Ruuskanen, P. Immonen, J. Nerg, J. Pyrhönen, Determining electrical efficiency of permanent magnet synchronous machines with different control methods, https://link.springer.com/ article/ 10.1007/s00202-011-0223-5.